

**RAPID SPECTRAL AND FLUX TIME VARIATIONS IN A SOLAR BURST OBSERVED
AT VARIOUS DM-MM WAVELENGTHS AND AT HARD X-RAYS**

**A. M. Zodi Vaz
P. Kaufmann
E. Correia
J. E. R. Costa**

INPE: Instituto de Pesquisas Espaciais
C.P. 515, 12.200-S. José dos Campos, SP, Brazil

E. W. Cliver

Air Force Geophysical Laboratory
Space Physics Division
Hanscom Air Force Base
Bedford, MA 01731

T. Takakura

Department of Astronomy
Faculty of Science
University of Tokyo
Bunkyo-ku, Tokyo 113, Japan

K. F. Tapping

Herzberg Institute of Astrophysics
National Research Council
Ottawa, Ontario KIA OR6, Canada

ABSTRACT

A solar burst was observed with high sensitivity and time resolution at cm-mm wavelengths by two different radio observatories (Itapetinga and Algonquin); with high spectral time resolution at dm-cm wavelengths by patrol instruments (Sagamore Hill); and at hard X-rays (HXM-Hinotori). At the onset of the major burst time structure there was a rapid rise in the spectral turnover frequency (from 5 to 15 GHz), in about 10s, coincident to a reduction of the spectral index in the optically thin part of the spectrum. The burst maxima were not time coincident at the optically thin radio frequencies and at the different hard X-ray energy ranges. The profiles at higher radio frequencies exhibited better time coincidence to the higher energy X-rays. The hardest X-ray spectrum (-3) coincided to peak radio emission at the higher frequency (44 GHz). The event appear to be build up by a first major injection of softer particles followed by other injections of harder particles. Ultrafast time structures were identified as superimposed to the burst emission at the cm-mm high sensitivity data and at X-rays, with predominant repetition rates ranging 2.0-3.5 Hz.

1. INTRODUCTION

The 4 November 1981, 1828 UT solar burst was observed simultaneously at eleven dm-mm wavelengths (0.4-44 GHz), by Sagamore Hill (AFGL, USA), Algonquin (HIA, Canada) and Itapetinga (INPE, Brazil) observatories, and at seven energy ranges at hard X-rays by HXM experiment on Hinotori satellite (28-375keV). Radio spectral data were obtained by Sagamore Hill (0.4-15 GHz), with very

good time resolution (1 spectrum/second). The Algonquin (10.6 GHz) and Itapetinga (22 and 44 GHz) data were obtained with high sensitivity, and high time resolution (limited here to 30 milliseconds). The hard X-ray data were analysed with a time resolution of 30 milliseconds in the lower energy channel (28-38 keV). Hard X-ray spectral indices were obtained every 5-10 seconds throughout the major burst duration.

2. TIME SPECTRAL VARIATIONS

In Figure 1 we show the flux time profiles, the time variations of the radio turnover frequency and of the spectral indices. The radio spectral index α in the optically thin part of the spectrum was obtained from the fluxes at 22 and 44 GHz, and defined as $F \propto f^\alpha$, where F is the flux and f the frequency. The X-ray data for the seven energy channels (28-375 keV) were fitted to a power law spectrum (defined as $I \propto E^\delta$, where I is the flux, E the photon energy, and δ is the power law spectral index) and to a thermal spectrum (defined as $I \propto (kT)^{-0.2} \times E^{-1.3} \times \exp(-E/kT)$, where T is the temperature and k is the Boltzmann constant). The main burst phase (1828-1829 UT) exhibited three predominant structures at the softer X-ray (28-38 keV) time profile, with peaks at 1828:19, 1828:27 and 1828:38 UT, respectively. The corresponding maxima at radio occurred approximately at 10.6 GHz, 22 GHz and 44 GHz, respectively. The 10.6 GHz time profile is considerably smoother, compared to the time profiles at higher frequencies. This trend was also observed at 7 GHz, by a patrol instrument operated at Itapetinga Radio Observatory (Takakura et al., 1983).

Before 1828 UT, there was a precursor which was more pronounced at lower frequencies, presenting a spectral turnover frequency at about 5 GHz. Between 1828:10 and 1828:20 UT (corresponding to the first X-ray structure), there was a very rapid increase of the turnover frequency up to ~15 GHz, simultaneously to a decrease of the 22-44 GHz spectral index from about -3.7 to -4.9. The rapid change in the radio turnover frequency is shown in more detail in Figure 2.

The remaining part of the main burst (1828:20 to 1828:50 UT) was characterized by an increase of the radio and X-rays spectral indices (hardening) and a slight decline of the radio turnover frequency.

After 1828:50 UT, there was a softening of the X-rays index, but the 22-44 GHz spectral index continued to increase, reaching values between -3.0 and -3.5.

The increase and decrease of the X-ray spectral index δ can also be described in terms of increase and decrease of the temperature, if we assume the thermal fit (shown by open circles in Fig. 1). The χ^2 test applied to the two fits indicated that the thermal spectrum was better fitted than the power law spectrum during the main phase of the burst (1828:13-1828:43 UT). However, it is known that multiple injections of power law populations can produce apparent better thermal fits.

The errors bars marked in the plot of the radio spectral index refer to the uncertainty in the estimates of the 22 and 44 GHz flux densities at the beginning of the burst. After 1828:10 UT, this error becomes negligible. There is still an uncertainty of 0.4 in the absolute value of α ,

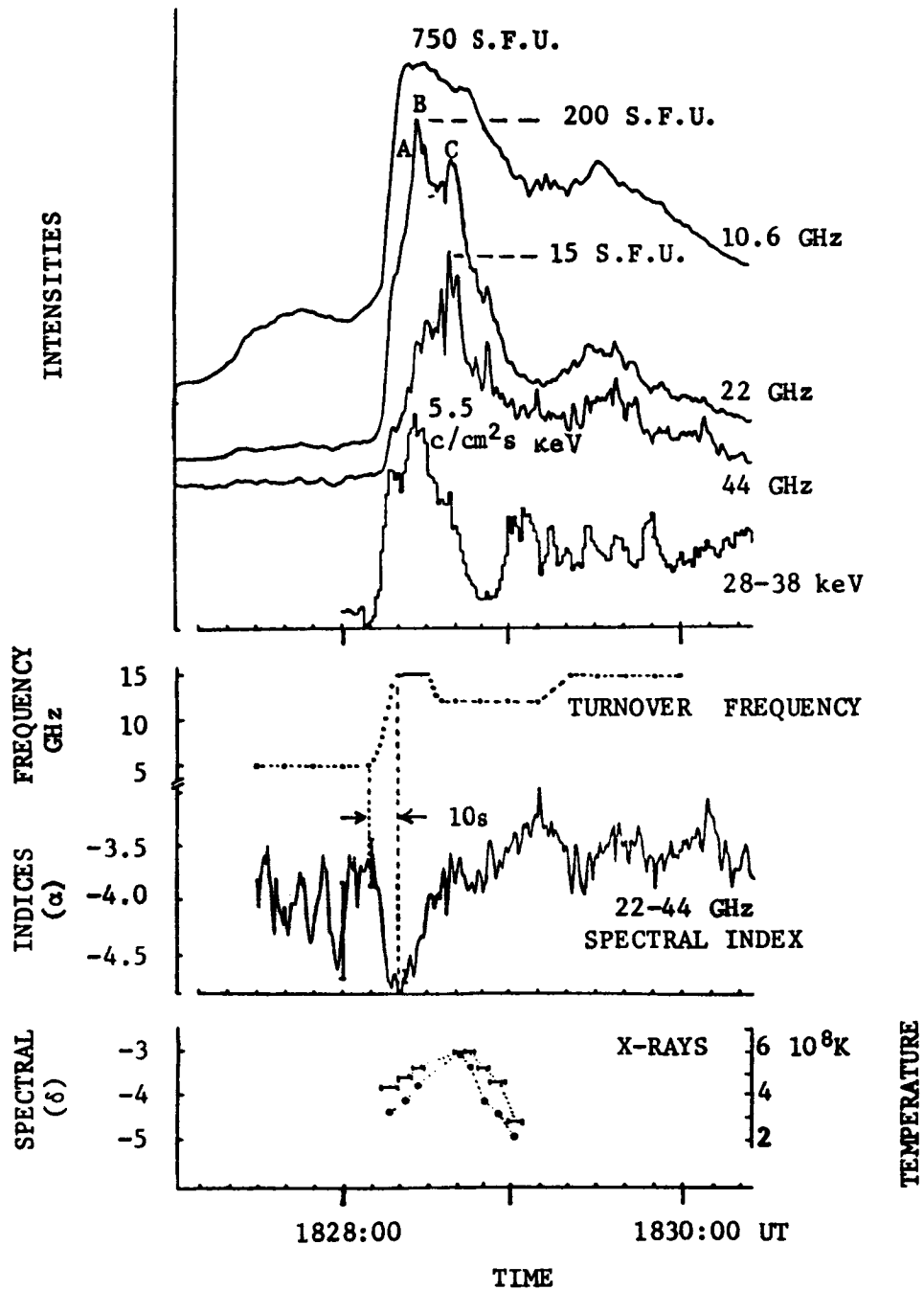


Figure 1 - Time profiles of the 4 November 1981, 1828 UT solar burst, including the intensities (the four plots at the top), the radio spectral turnover frequency, and the radio spectral index (α) at the optically thin part of the spectrum (22-44 GHz). At the bottom, the X-rays power law spectral index (δ), in time segments corresponding to the intervals they were obtained (ordinates at the left), and the X-rays thermal fit temperatures, in circles (ordinates at the right).

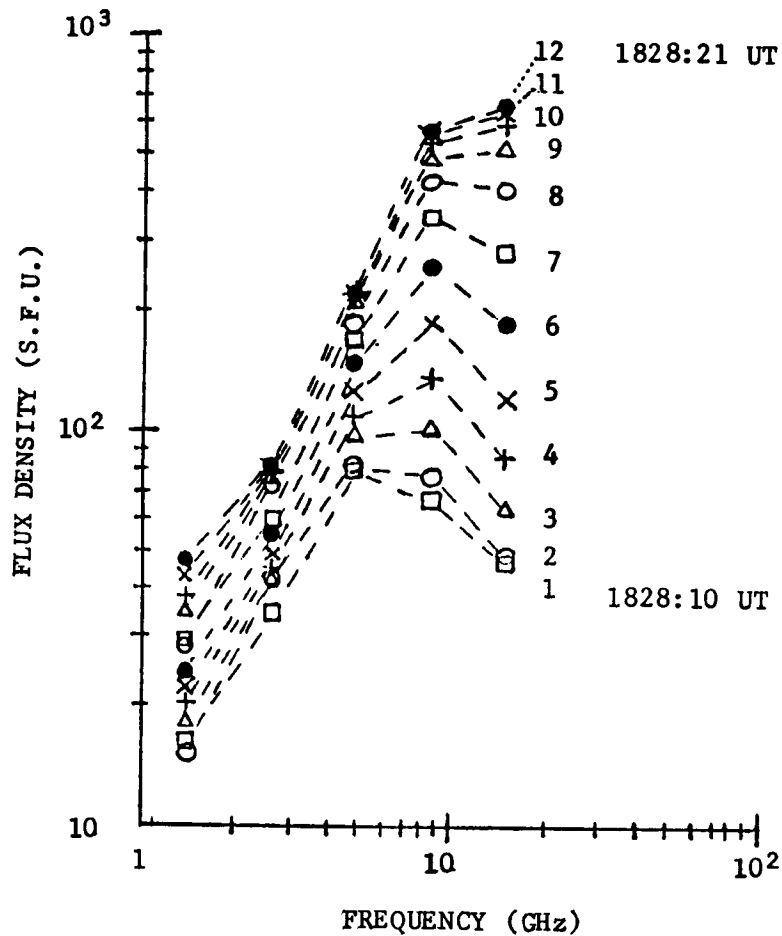


Figure 2 - The rapid variation of the turnover frequency between 1828:10 and 1828:21 UT, is shown by successive spectra, obtained every second, labeled 1-12, at five dm-cm frequencies by Sagamore Hill Radio Observatory (AFGL). The last three spectra (10, 11 and 12) are essentially identical. The shift in the turnover frequency (5-15 GHz) occurred in less than 10s.

due to the uncertainty of about 20% in the calibration of the 22 and 44 GHz flux scales. However, this effect is meaningless when we consider the time variation of α .

Figure 3 shows the X-rays time profiles at the six higher energy channels. There is a gap in the data between 1828:28 UT and 1828:37 UT, but it can be seen that the first structure at 1828:19 UT was more pronounced at the lower energies, while the third structure (1828:38 UT) was more pronounced at higher energies. As shown in Figure 1, the 44 GHz maximum occurred at the time of the third X-ray structure.

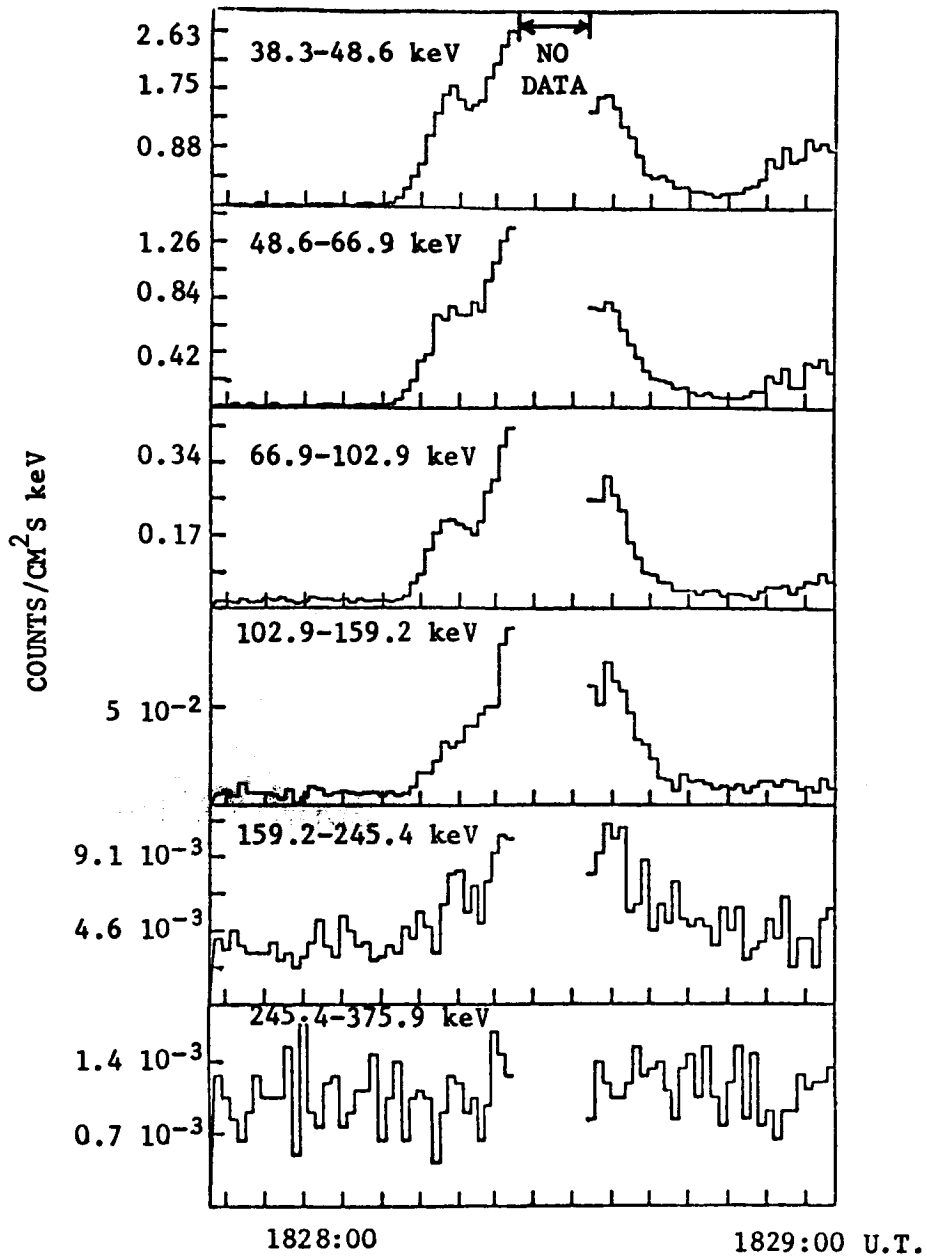


Figure 3 - X-rays time profiles at the harder energy ranges obtained by HXM experiment on board of the Hinotori satellite. The softer energy channel (28-38 keV) is shown in Figure 1. Note that the 22 GHz time profile (Figure 1) fits better to the 102.9-159.2 keV channel, while the 44 GHz time profile (Figure 1) fits better to the 159.2 - 245.4 keV channel.

3. SUB-SECOND TIME STRUCTURES

Time expanded sections of this burst reveal that sub-second pulsations were present in the radio and X-rays time profiles. This phenomenon was studied by Takakura *et al.* (1983), in the same burst. Their analysis, however, was restricted to two time intervals (of 2s), and the Algonquin 10.6 GHz high sensitivity data were not available. Figure 4 reproduces an expanded section of the original 22 GHz and 44 GHz time profiles obtained by two independent radiometers at the focus of the Itapetinga 45ft antenna. We have analysed in more detail three 4.3s intervals across the main burst structure, labeled A, B and C in Figure 1. The technique used was the subtraction of the data from running means, as described in the caption of Figure 5.

SECTION C

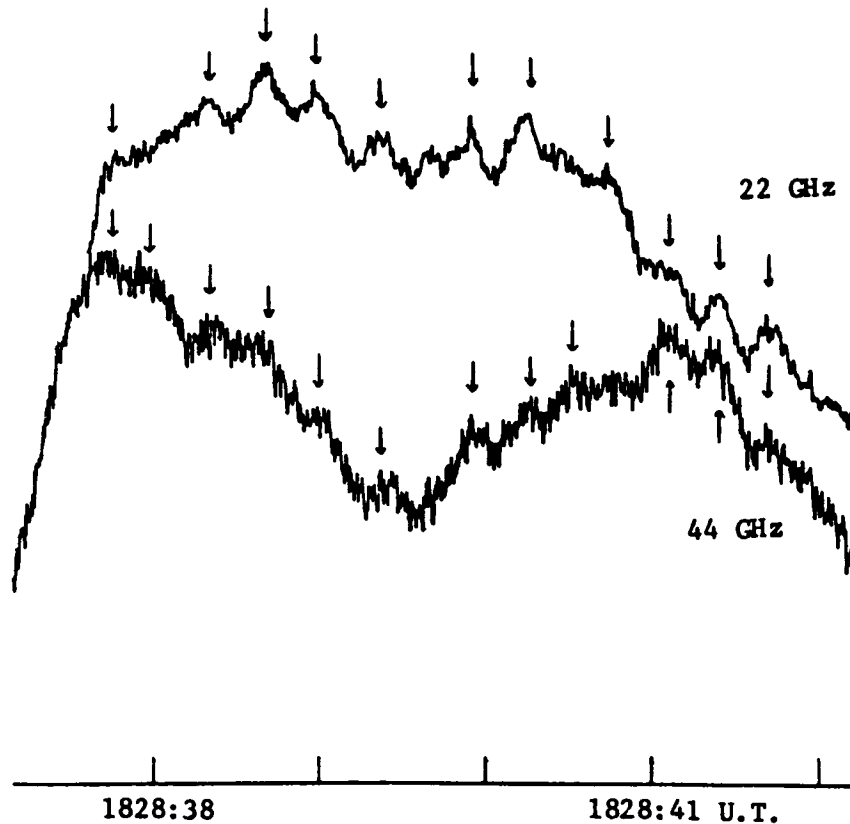


Figure 4 - Example of 22 and 44 GHz raw data without any filtering or processing, obtained for Section C (Figure 1). Superimposed fast structures are identified at the two frequencies by arrows. The mean time interval between consecutive well defined pulses is of about 0.3s, corresponding to a repetition rate of about 3.3 Hz. This burst section is analysed again in Figure 8, together with 10.6 GHz and hard X-rays data.

Figure 5 shows a sample of the uncertainties in fluctuations outside the burst period of time. They include the system noise and other fluctuations, which were due to excess noise at the data acquisition system (at 22 and 44 GHz), or to fluctuations of unknown origin (at 10.6 GHz). The figures 6-8 show the burst sections A,B and C, which compared to Figure 5 indicate clearly the presence of sub-second pulsations at the three radio frequencies and at 28-38 keV X-rays. The figure captions describe further details of the analysis. The repetition rates of the superimposed fast pulses ranged from 2-3.5 Hz. The subsecond pulses at 10.6 GHz were particularly pronounced at the main structures A and B, reducing substantially at structure C, as well as in the remaining part of the event. The relative amplitudes of the subsecond pulses at the corresponding maxima were of 0.7% (10.6 GHz), 3% (22 GHz), 7% (44 GHz), and 23% (at 28-38 keV X-rays). This result confirm the tendency of having better defined sub-second structures for higher mm-wave frequencies (Kaufmann et al., 1984; 1985).

We still observe that the time correlation between pulses at different radio frequencies and at X-rays is often poor or nonexistent. The nature of this effect is not known, and deserves further analysis. One possibility might be that the fine time structures were not entirely resolved. Convolution effects may have produced the observed "ripple" structures, differently at the three radio frequencies and at X-rays (Brown et al., 1983; Loran et al., 1985).

The Fourier analysis techniques were highly criticized in the present Workshop, when applied to pulsed phenomena which are not strictly periodic. In spite of these restrictions, we obtained Fourier spectra for several sections throughout the burst duration. One example is shown in Figure 9, corresponding to the 4.3s burst section B (Figure 7). The results indicate the presence of several frequencies, with different relative amplitudes for different radio frequencies and hard X-rays, and confirm some repetition rates common to the four time profiles of section B (Figure 7).

4. CONCLUDING REMARKS

The impulsive burst may be interpreted as consisting of several major overlapping acceleration phases. In a first phase, the accelerated population of electrons are predominantly softer in energy. The sudden increase in turnover frequency may be attributed to the increase in density of accelerated electrons. The excess of particles with softer energies causes the decrease in the radio spectral index in the optically thin part of the spectrum. The following phases corresponded to a hardening of the radio and X-ray spectra, exhibiting peak emission, first at 22 GHz, followed by the peak at 44 GHz, nearly 20 seconds after the first phase. The phases appear to be build up of multiple rapid injections, which may also be superimposed or mixed up, producing complex power spectra or repetition rate frequencies.

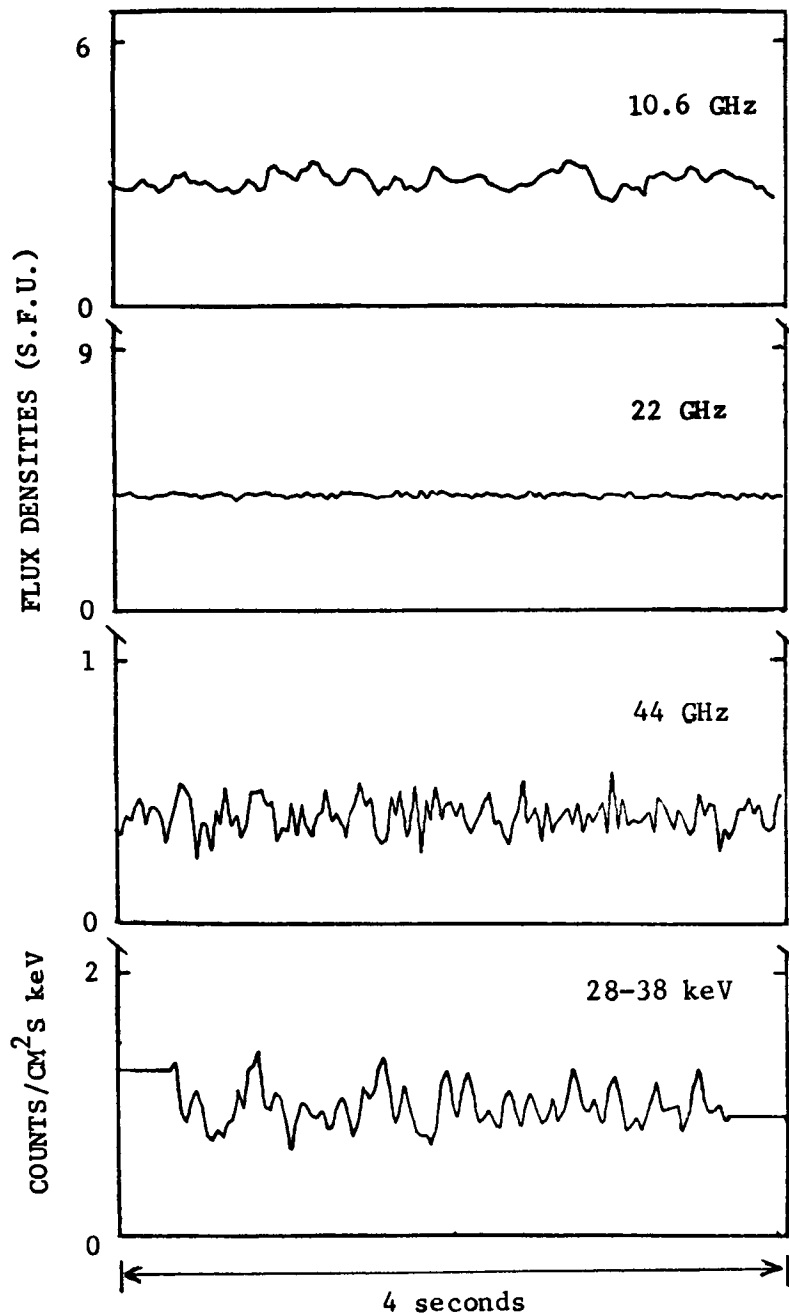


Figure 5 - 4 seconds of data obtained when tracking the active region previously to the event, in order to show the level of uncertainties in fluctuations at 10.6 GHz (Algonquin), 22 and 44 GHz (Itapetinga) and 28-38 keV (HXM-Hinotori). The plots were obtained by subtracting the data from 700 ms running mean baseline. The radio data was time integrated in 30 ms, in order to become comparable to the X-ray time resolution. The X-ray data was further smoothed out by a 90 ms running mean (this technique keeps the 30 ms time resolution).

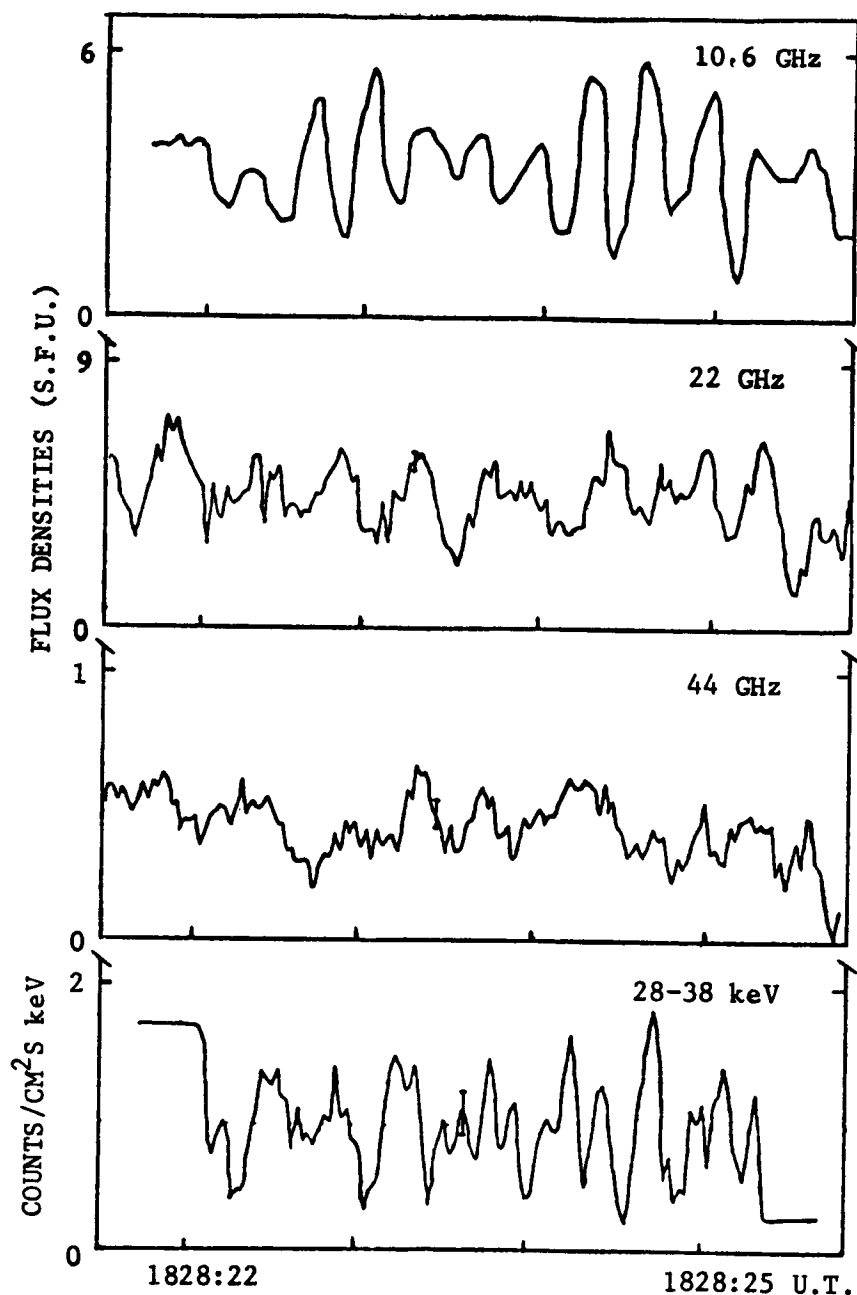


Figure 6 - 4.3 seconds interval of burst section A (Figure 1), obtained in the same scales and data reduction techniques used in the plots of Figure 5. The superimposed fast structures are clearly enhanced at the three radio frequencies and at hard X-rays. The error bars at 22 and 44 GHz take into account the increase in system temperature with the burst emission. Although there is a good correspondence between 22 and 44 GHz pulses, some of the pulses at 10.6 GHz and at X-ray are not well correlated. The time intervals between two significant and consecutive pulses are nearly similar in the four plots, varying between 0.28s and 0.36s, corresponding to repetition rates ranging between 2.8 Hz and 3.5 Hz.

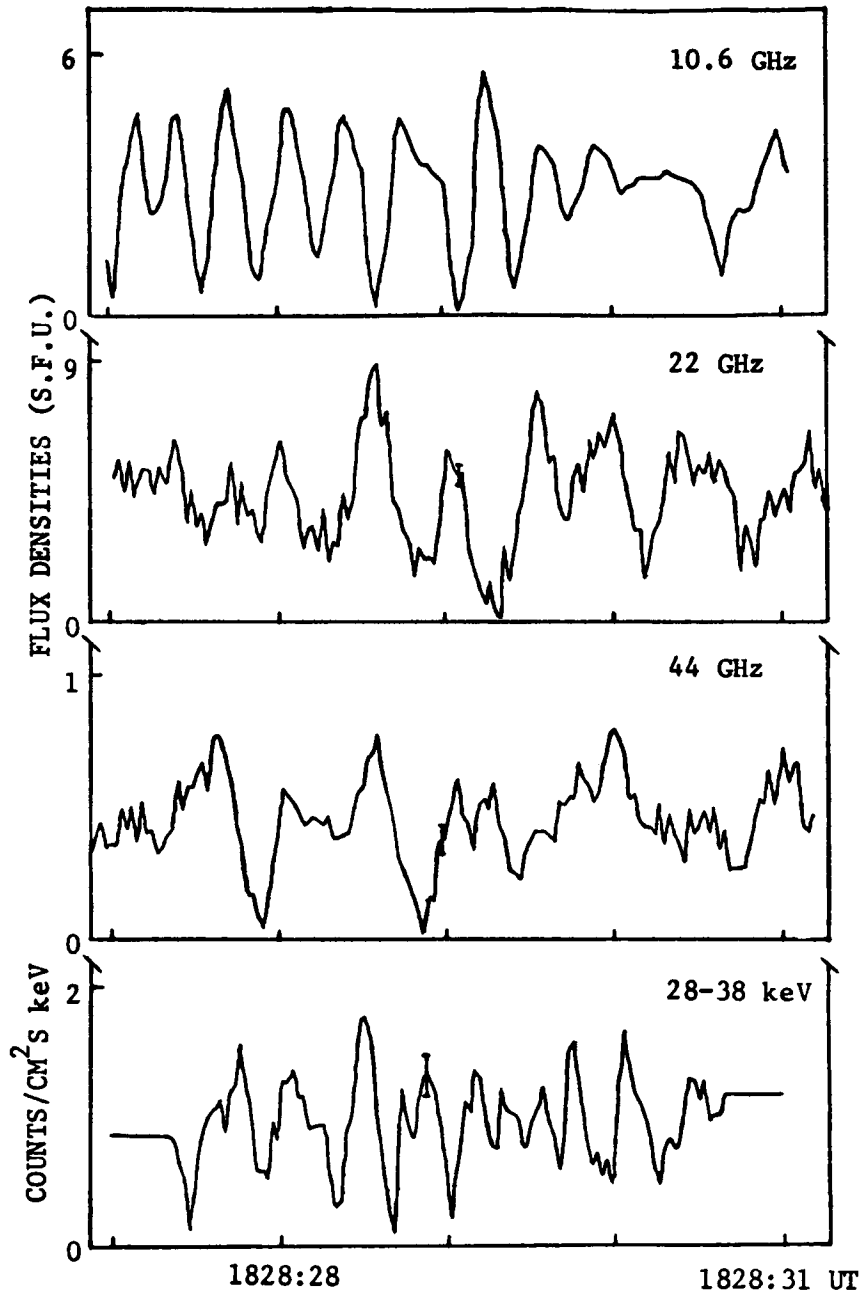


Figure 7 - 4.3 seconds interval of burst section B (Figure 1), obtained in the same conditions of the Figures 5 and 6. Fourier spectra of this section were also determined and are shown in Fig. 9. Like in section A (Figure 6), the time intervals between consecutive pulses denote the presence of more than one frequency, of about 2, 2.5 and 3.5 Hz. The Fourier spectra of Figure 9 also show these components, with different relative importance at the different radio frequencies and at hard X-rays.

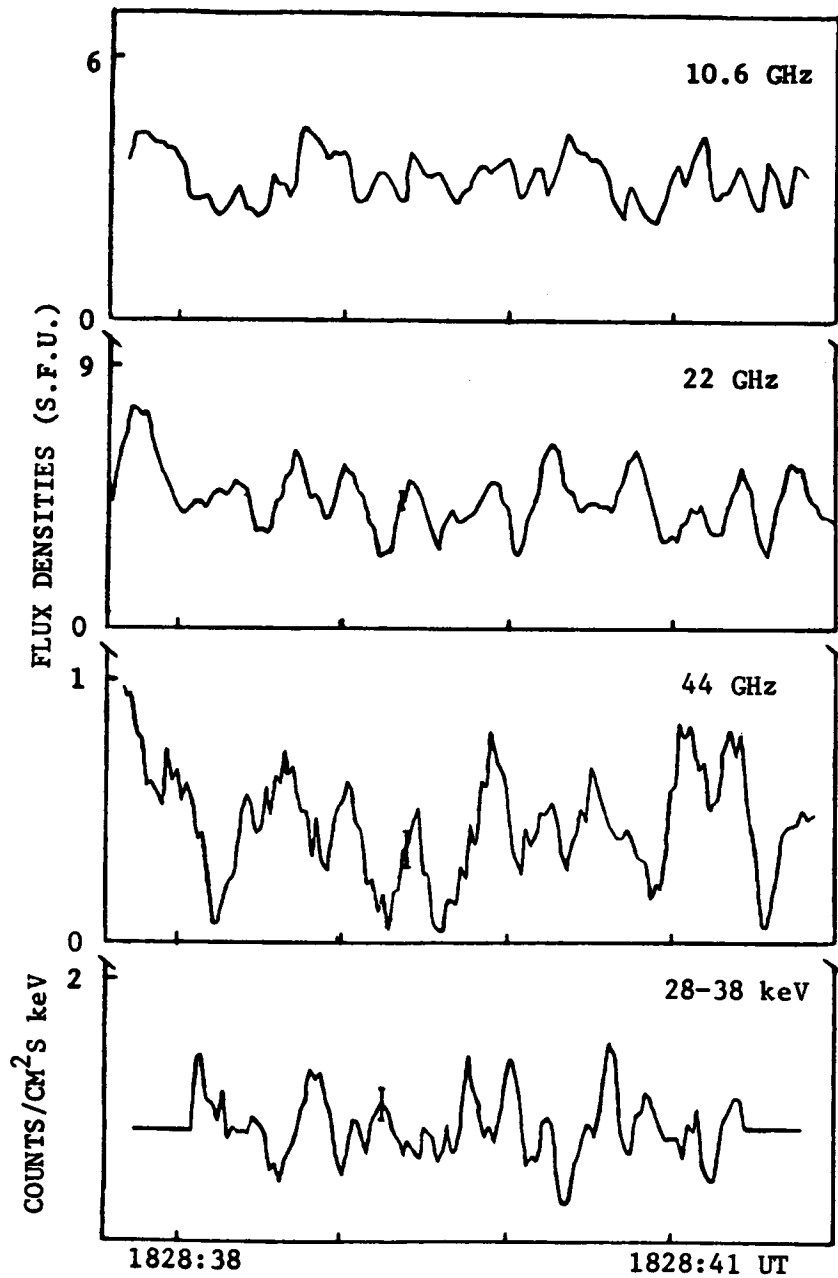


Figure 8 - 4.3 seconds interval of burst section C (Figure 1), obtained in the same conditions of the previous sections (Figure 5-7). In this section the fast pulses are better seen at 22 and 44 GHz. The original data at these frequencies were shown in Figure 4 and display the same structures.

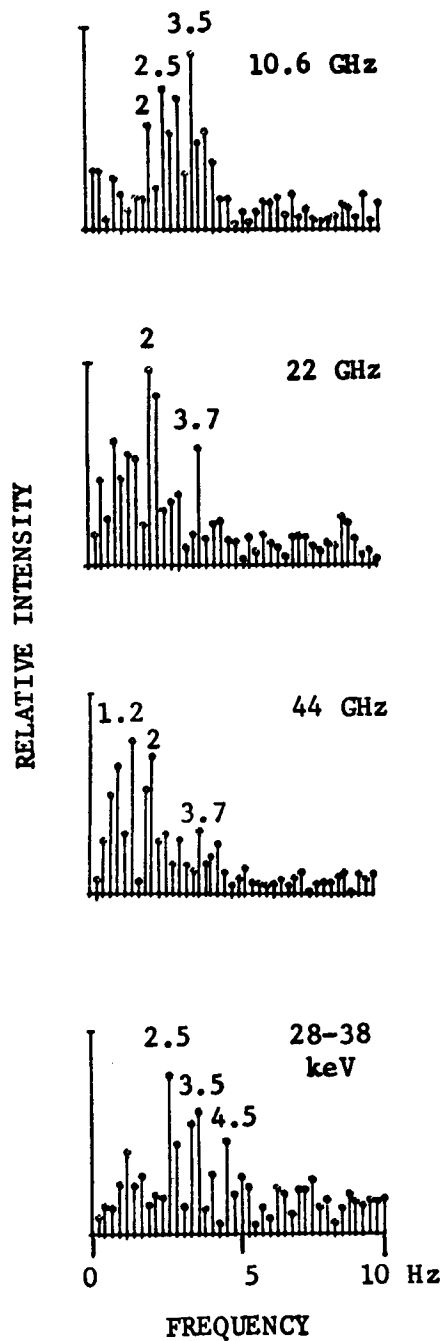


Figure 9 - Fourier spectra obtained for burst section B, about 4s in duration, which was shown expanded in Figure 7. The predominant time structures exhibit repetition rates of about 2.0-2.5 Hz and 3.5 Hz at the three radio frequencies and at hard X-rays, with different relative intensities.

Acknowledgements

This research was partially supported by the Brazilian research agency FINEP. INPE operates CRAAM and Itapetinga Radio Observatory. One of the authors (PK) is Guest Investigator on NASA-SMM Project.

REFERENCES

- Brown, J.C., MacKinnon, A.L., Zodi, A.M., and Kaufmann, P.: 1983, *Astron. Astrophys.*, 123, 10.
- Kaufmann, P., Correia, E., Costa, J.E.R., Dennis, B.R., Hurford, G.J., and Brown, J.C.: 1984, *Solar Phys.*, 91, 359.
- Kaufmann, P., Correia, E., Costa, J.E.R., Zodi Vaz, A.M., and Dennis, B.R.: 1985, *Nature*, 313, 380.
- Loran, J.M., Brown, J.C., Correia, E., and Kaufmann, P.: 1985, *Solar Phys.*, 97, 363.
- Takakura, T., Kaufmann, P., Costa, J.E.R., Degaonkar, S.S., Ohki, K., and Nitta, N.: 1983, *Nature*, 302, 317.